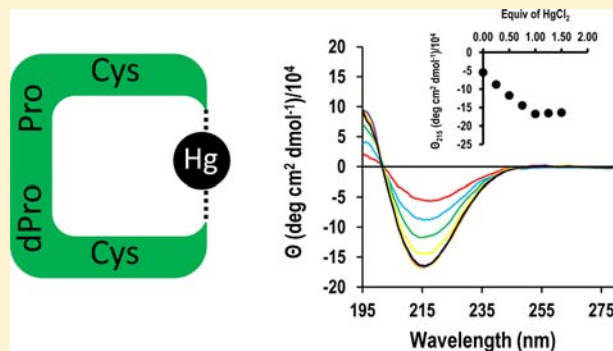


Design of a Peptidic Turn with High Affinity for Hg^{II}Sara Pires,[†] Jelena Habjanič,[†] Murat Sezer,[†] Cláudio M. Soares,[†] Lars Hemmingsen,[‡] and Olga Iranzo^{*†}[†]Instituto de Tecnologia Química e Biológica, Universidade Nova de Lisboa, Avenida da República, 2780-157 Oeiras, Portugal[‡]Department of Chemistry, University of Copenhagen, Universitetsparken 5, 2100 København Ø, Denmark

Supporting Information

ABSTRACT: A four amino acid peptide containing the β -turn template *d*Pro-Pro in the middle and two cysteines (Cys) in the terminal positions (CdPPC) has been synthesized and its mercury(II) coordination properties studied using different spectroscopic methods. The UV-vis, CD, ^{199m}Hg PAC, and Raman spectroscopic studies indicate the binding of Hg^{II} to the two Cys, forming the dithiolatemercury(II) complex Hg-(CdPPC). Electro spray ionization mass spectrometry corroborates the 1:1 complex formation. A log *K* = 40.0 was determined for the formation constant of the Hg(CdPPC) complex using competition potentiometric studies. Replacement of the *d*Pro-Pro motif by a Pro-Pro unit generated a peptide (CPPC) capable of forming a similar species [Hg(CPPC)] but showing a lower affinity for Hg^{II} (at least 3–3.5 orders of magnitude lower). The introduction of the *d*Pro-Pro motif is crucial to induce the folding of the CdPPC peptide into a β -turn, preorganizing the two Cys for mercury(II) coordination. While the simple *d*Pro-Pro unit mimics the overall preorganization achieved by the protein scaffold in metalloproteins containing the conserved metal ion chelation unit CXXC, the high thiophilicity of this metal stabilizes the final complex in a wide pH range (1.1–10). Using computational modeling, the structures of two conformers for Hg(CdPPC) have been optimized that differ mainly in the orientation of the plane containing S–Hg–S with respect to the anchoring C atoms.



The introduction of the *d*Pro-Pro motif is crucial to induce the folding of the CdPPC peptide into a β -turn, preorganizing the two Cys for mercury(II) coordination. While the simple *d*Pro-Pro unit mimics the overall preorganization achieved by the protein scaffold in metalloproteins containing the conserved metal ion chelation unit CXXC, the high thiophilicity of this metal stabilizes the final complex in a wide pH range (1.1–10). Using computational modeling, the structures of two conformers for Hg(CdPPC) have been optimized that differ mainly in the orientation of the plane containing S–Hg–S with respect to the anchoring C atoms.

INTRODUCTION

The short amino acid sequence Cys-X-X-Cys (CXXC) is a highly conserved chelating unit in biological systems. It is found in the metal binding site of a wide variety of metalloproteins,^{1–4} among them those involved in the bacterial mercury detoxification system (MerP)⁵ and the copper transport systems from humans (HAH1),⁶ yeasts (Atx1),⁷ and bacteria (CopZ).⁸ This short chelating unit is mainly found in loops. It has high flexibility and thus shows structural diversity depending on the coordination geometry of the metal center and the nature of the X amino acids.^{2,4,9} In all cases though, the overall structure of the protein scaffold helps to organize the loop and the Cys residues for proper metal binding.

Linear and cyclic peptides containing this binding motif have been designed as models for these loops, and their metal ion coordination properties have been investigated. The results show that they coordinate Hg^{II} with high affinity through the two Cys amino acids, forming dithiolate complexes (Hg-(Cys)₂). Opella and co-workers synthesized three 18-residue linear peptides derived from the metal binding loop of MerP (TLAVPGMTCAACPITVKK) known to have structural and binding characteristics similar to those of the full MerP protein.^{2,10,11} These studies showed how the location of the binding residue Cys in the linear sequence determines the strength of Hg^{II} binding (CCAA > CAAC (native) ≫ CACA). Cyclic and linear (acyclic) 10-residue peptides containing the binding sequence *MTCSGCS* of the Atx1 metallochaperone

have been developed by the research group of Delangle and shown to coordinate Hg^{II} with high affinity.^{12,13} In this case, the stability of the mercury(II) cyclic peptide complex was up to 2 orders of magnitude higher than that observed for the linear counterpart because of preorganization of the Cys residues. In such small peptides, the use of the β -turn-inducing XPGX motif to cycle the scaffold has been fundamental in preorganizing the two Cys residues in a loop structure for proper metal binding, increasing thus its Hg^{II} affinity. Pecoraro and co-workers showed that the introduction of the CXXC motif and the less common binding site CXXXC into the de novo designed 30-residue TRI peptide family generated the complexes [Hg-(Cys)₃]⁻ and [Hg(Cys)₄]²⁻. The different mercury(II) coordination numbers that were observed resulted from self-association of these peptides into two- or three-stranded coiled coils.¹⁴

All of these studies reveal that peptides have very attractive features for the design of metal-coordinating ligands. Among these features is their modular nature, which allows modification of their structure and spatial distribution of functional groups, as well as their accessible synthesis by well-established solid-phase methodology. Nonetheless, small peptides usually lack structure in solution. Therefore, the introduction of specific sequences known to induce features of

Received: April 19, 2012

Published: October 17, 2012

secondary structure becomes fundamental to obtaining the desired rearrangement of the binding units. This is achieved in native systems by the overall protein scaffold. In small peptides, one of the strategies most employed to obtain structures with the potential to adopt folding is the introduction of amino acid sequences known to induce a β turn, usually a four amino acid sequence containing a Pro (XPXX). In addition to the work by Delangle,^{12,13,15} this approach has been used by different research groups in the design of both acyclic and cyclic peptides with specific metal ion coordination properties.^{16–18} Nonetheless, these sequences by themselves were not enough to induce a specific structure in the acyclic apopeptides. Another template reported to induce β turns is the dipeptide *d*Pro-Pro. This simple unit has very well-known β -turn-inducing properties,^{19–21} and it has been employed to induce β -sheet and β -hairpin loop formation upon introduction in short amino acid sequences.^{22–25}

Herein, we report a tetrapeptide Ac-Cys-*d*Pro-Pro-Cys-NH₂ (CdPPC) containing the motif *d*Pro-Pro to preorganize two Cys residues for Hg^{II} binding. The mercury(II) coordination properties of this peptide have been studied using potentiometric and different spectroscopic techniques. To investigate the effect of reversing the stereochemical configuration of the first proline, known to be a strong turn determinant when L-amino acids are used,¹⁹ its metal ion coordination properties were compared with those of the peptide Ac-Cys-Pro-Pro-Cys-NH₂ (CPPC). The results show that both peptides bind Hg^{II} in a similar way. However, competition experiments with Cys reveal that CdPPC, capable of adopting a predefined secondary structure in solution, has higher affinity constants for Hg^{II} than CPPC.

RESULTS

Peptide Synthesis. The peptides CdPPC and CPPC were obtained by solid-phase peptide synthesis using a microwave-assisted peptide synthesizer (CEM Liberty). Standard Fmoc chemistry,²⁶ MBHA Rink amide resin, and the HBTU/HOBt/DIEA coupling mixture were employed. The peptide was purified by reverse-phase high-performance liquid chromatography (HPLC) using the solvent system water/acetonitrile/trifluoroacetic acid and characterized by electrospray ionization mass spectrometry (ESI-MS; Figure S1 in the Supporting Information, SI). The CdPPC and CPPC peptides are acetylated at the N-terminus and amidated at the C-terminus.

Spectroscopic Studies. *Ultraviolet–Visible (UV–Vis) Absorption Spectroscopy.* Formation of the mercury(II) complex with the peptides CdPPC and CPPC was studied by UV–vis absorption spectroscopy, monitoring the ligand-to-metal charge-transfer (LMCT) band for Hg–S bonds observed in the UV region.²⁷ In order to distinguish the LMCT band from the peptide's UV absorption, the background spectrum of the peptide in the absence of metal was subtracted. Here, only the difference spectra after subtraction of the peptide contribution are presented. The extinction coefficients were calculated on the basis of the total peptide concentration.

i. Binding of Hg^{II} to CdPPC and CPPC. In Figure 1, the difference absorption spectra for the titration of Hg^{II} into a buffered solution of the CdPPC peptide at pH 7.6 are shown. The steady increase in the absorption band centered at 220 nm abruptly plateaus at 1 equiv of Hg^{II}, indicating the formation of a mercury(II) complex with 1:1 peptide/mercury(II) stoichiometry (Hg(CdPPC)) and with an extinction coefficient of 11400 M⁻¹ cm⁻¹. These values are in agreement with reported

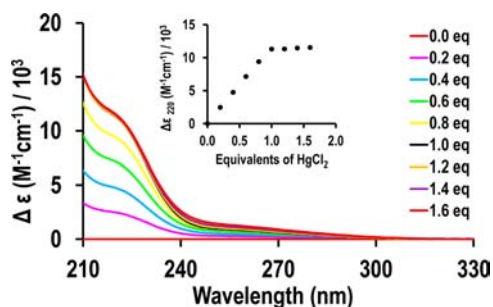


Figure 1. Titration of HgCl₂ into a solution of CdPPC (25 μM) at pH 7.6 (20.0 mM phosphate buffer) followed by UV–vis difference spectroscopy. The inset shows the titration curve obtained by plotting the change in the extinction coefficient, $\Delta\epsilon$, at 220 nm versus equiv of metal added.

data for linear dithiolatemercury(II) complexes.^{13,27–29} Similar behavior was observed for the binding of Hg^{II} to the CPPC peptide under the same experimental conditions (Figure S2 in the SI; absorption band centered at 222 nm). However, after 1 equiv of Hg^{II}, the absorbance at 250 nm increased, which may indicate the formation of polymetallic mercury(II) species. The UV–vis spectrum obtained when 1 equiv of Hg^{II} was added to a solution containing an equimolar amount (25 μM) of peptides is reported in Figure 2.

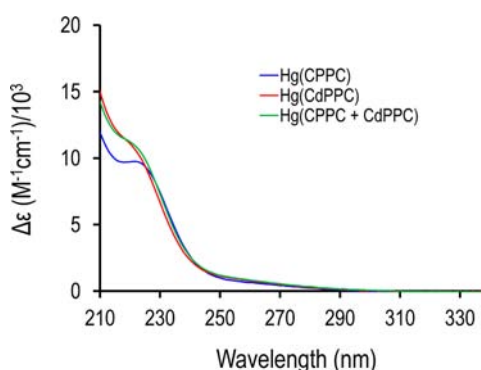


Figure 2. UV–vis spectrum (green line) obtained after the addition of 1 equiv of HgCl₂ into a solution containing CdPPC (25 μM) and CPPC (25 μM) at pH 6.0 (20.0 mM phosphate buffer). For comparison, the spectra corresponding to the mercury(II) complexes of CPPC (blue) and CdPPC (red) are included.

ii. pH Dependence and Hg(CdPPC) Complex Stability. The pH of solutions containing 25 μM peptide and 1 equiv of Hg^{II} was varied from 1.1 to 10.0, and the UV–vis spectra recorded show no significant changes over the pH range studied (Figure S3 in the SI). The experimental data show that the mercury(II) complex of both peptides is also formed at low pH values and is stable up to pH 10.0. The same experiment in the absence of Hg^{II} showed an increase in absorbance in the spectral window from 230 to 270 nm when the pH was higher than 8.0, indicating formation of the thiolates. The absence of this band in the presence of Hg^{II} confirms its coordination to Cys. The stability over time of the mercury(II) complex of the CdPPC peptide at different pH values (2.5, 7.4, and 9.0) was monitored by recording periodically the UV–vis spectra of the different solutions. No significant changes were observed within 36 days.

Circular Dichroism (CD) Spectroscopy. To determine if the peptides in the absence of Hg^{II} have any secondary structure

features in aqueous solution, their CD spectra were recorded in the far-UV spectral region. The CD spectrum of a solution containing 10 μM CdPPC at pH 7.4 is presented in Figure 3

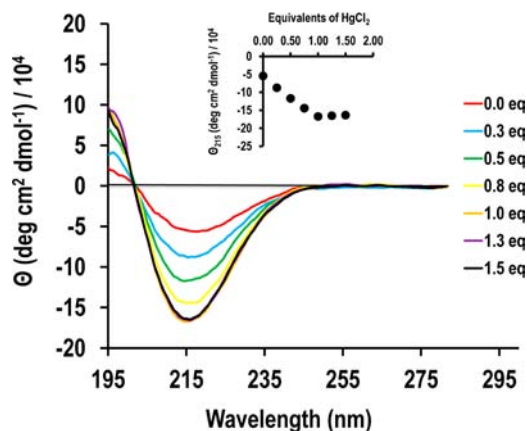


Figure 3. Titration of HgCl_2 into a solution of CdPPC (10 μM) at pH 7.4 (unbuffered solution) followed by CD spectroscopy. The inset shows the titration curve obtained by plotting the change in the molar ellipticity at 215 nm versus equiv of metal added.

and shows the characteristic signature of a β -turn and a β -hairpin loop (absorbance maximum at 215 nm with negative ellipticity).³⁰ However, under the same experimental conditions, CPPC presents a CD spectrum (Figure S4 in the SI) reminiscent of a random-coil structure (unfolded peptide) with an absorbance maximum at 203 nm and negative ellipticity.

i. Binding of Hg^{II} to CdPPC and CPPC. The addition of Hg^{II} to the CdPPC solution produced an increase in the negative ellipticity of the band observed for the peptide alone, reaching a plateau at 1 equiv of Hg^{II} . This is consistent with the formation of a 1:1 peptide/mercury(II) species. An isodichroic point is observed at 201.5 nm, suggesting the formation of a unique species. For the CPPC peptide, the addition of up to 1 equiv of Hg^{II} produced a decrease in the absorbance at 203 nm with a concomitant increase at 216 nm (Figure S4 in the SI). The spectrum at 1 equiv of Hg^{II} presents the same features as those observed for the CdPPC peptide but with much lower intensity (Figure 4, blue and red solid lines). When more equivalents of Hg^{II} were added to CPPC, the CD signal decreased (Figure S4

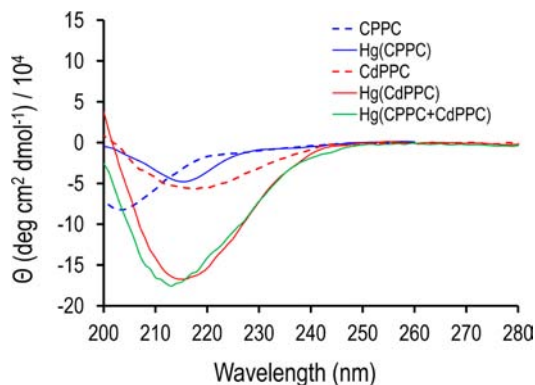


Figure 4. CD spectrum (green line) obtained after the addition of 1 equiv of HgCl_2 into a solution containing CdPPC (10 μM) and CPPC (10 μM) at pH 6.0 (20.0 mM phosphate buffer). For comparison, the spectra corresponding to the mercury(II) complexes of CPPC (blue) and CdPPC (red) are included.

in the SI). Well-defined isodichroic points were not observed. The addition of 1 equiv of Hg^{II} to a solution containing equimolar amounts of CdPPC and CPPC at pH 6.0 generated the CD spectrum shown in Figure 4 (green solid line).

ii. pH Dependence. The pH of a solution containing 10 μM CdPPC and 1 equiv of Hg^{II} was varied from 3.0 to 10.0, and the CD spectra recorded show no significant changes over this pH range (Figure S5 in the SI). This result corroborates the pH insensitivity observed by UV-vis spectroscopy. No oxidation of Cys at high pH was observed because no CD signal appears in the region 270–300 nm where the n-to- σ^* S–S transition band is expected.^{31,32}

^{199m}Hg Perturbed Angular Correlation (PAC) Spectroscopy. ^{199m}Hg PAC spectroscopy was used to determine the mercury(II) coordination geometry of the mercury(II) complex of CdPPC. Figure 5 shows the Fourier transforms of the ^{199m}Hg

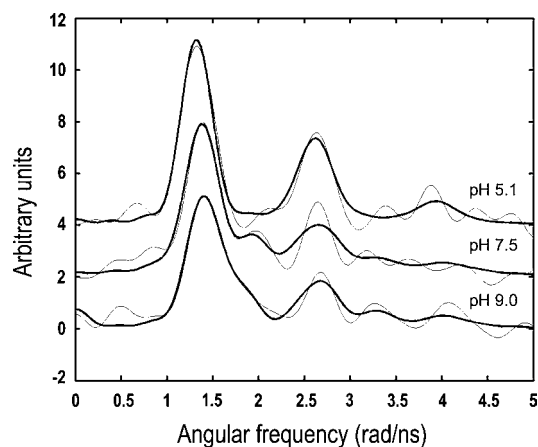


Figure 5. ^{199m}Hg PAC spectra of frozen (77 K) solutions containing 25 μM peptide, 22.5 μM $\text{Hg}(\text{CH}_3\text{COO})_2$, and 35.0 mM appropriate buffer at different pH values. The thin lines represent the Fourier transform of the experimental data, and the bold lines represent the fit. Two NQIs were included in the fit, but only the parameters for the dominating species are presented in Table 1 because it was not possible to analyze the second NQI unambiguously.

PAC spectra recorded for CdPPC and Hg^{II} at a peptide/mercury(II) ratio of 1:0.9 and at different pH values. The data were analyzed as described in the Experimental Section, and the parameters fitted to these PAC data (ν_Q , η , δ , $1/\tau_Q$, A , and χ_r^2) are reported in Table 1. Only one nuclear quadrupole

Table 1. Parameters Fitted to the ^{199m}Hg PAC Data^a

pH	Hg^{II} (equiv)	ν_Q (GHz)	η	$\delta \times 100$	$A \times 100$	χ_r^2
5.1	0.9	1.39(1)	0.09(5)	4.8(8)	15.8(7)	0.73
7.5	0.9	1.42(2)	0.19(4)	11(1)	17.2(9)	0.71
9.0	0.9	1.45(2)	0.21(4)	10(1)	15.3(7)	0.77

^aNumbers in parentheses are the standard deviations of the fitted parameters.

interaction (NQI) was found for the experiment at pH 5.1. This set of signals corresponds to $\nu_Q = 1.39$ GHz and $\eta = 0.09$. These fitted PAC parameters compare reasonably well with the literature data for a model compound with a two-coordinated, almost linear S–Hg–S structure, although ν_Q is slightly lower ($[\text{Hg}(\text{Cys})_2]$, $\nu_Q = 1.41$ GHz and $\eta = 0.15$).³³ When the pH is increased to 7.5, the spectrum changes slightly compared to pH 5.1. Nonetheless, the data could be fitted with one NQI with

PAC parameters ($\nu_Q = 1.42$ GHz and $\eta = 0.19$) that also correspond to a distorted linear HgS_2 coordination geometry. A small shoulder is observed to the right of the major peak (about 1.9 Grad s^{-1}). This may indicate the existence of a second NQI. However, it was not possible to unambiguously analyze this potential second NQI, which represents up to about 25% of the total signal. A similar spectrum was obtained at pH 9.0 ($\nu_Q = 1.45$ GHz and $\eta = 0.21$). Overall, at pH values 7.5 and 9.0, the PAC signal is dominated by a NQI that corresponds to a distorted dithiolatemercury(II) complex $[\text{HgS}_2]$.

Raman Spectroscopy. Raman and UV resonance Raman spectroscopies have proven to be powerful tools for characterization of mercury thiolate complexes of the $\text{Hg}(\text{S-R})_n$ type.^{34–38} In particular, a strong band in the region between 180 and 400 cm^{-1} , mainly attributable to the symmetric Hg–S stretching vibration (ν_s), was shown to be a sensitive probe of the coordination pattern of the Hg center.^{36,37} The exact position of this band strongly depends on the chemical constitution of the thiolate ligands (R),^{36,37} and, to an even greater extent, on the number of coordinating thiolates (n).^{36–38} Increasing the thiolate coordination number leads to increasing Hg–S bond length³⁴ and decreasing energy of the Raman bands involving the $\nu_s(\text{Hg–S})$ mode.^{35–38} While two-coordinated complexes are reported to display $\nu_s(\text{Hg–S})$ bands above 300 cm^{-1} ,³⁸ the position of this band lies between 200 and 300 cm^{-1} for three-coordinated complexes³⁶ and is even further decreased in four-coordinated complexes.^{35,38} Here Raman difference spectroscopy was employed to identify the band(s) that originate from the vibrational modes that involve the Hg center. In the $[\text{Hg}(\text{CdPPC}) - \text{CdPPC}]$ difference spectrum (Figure 6, trace c), a single broad band at 325 cm^{-1}

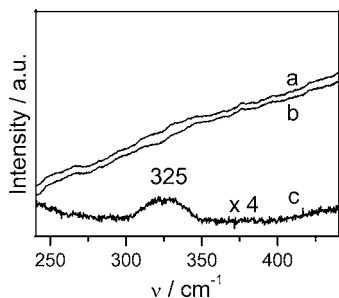


Figure 6. Raman spectra of (a) $\text{Hg}(\text{CdPPC})$ and (b) peptide CdPPC and (c) difference Raman spectrum (a – b), measured from lyophilized samples at 83 K, 413 nm excitation, 7.5 mW laser power, and 60 accumulation time. A total of 80 spectra were added for spectra a and b, respectively.

was observed in lyophilized solid samples. On the basis of the data reported in the literature, this signal was assigned to $\nu_s(\text{Hg–S})$ of a bis-Cys-coordinated mononuclear mercury complex.^{34–38} In frozen solution samples, this band upshifts to 329 cm^{-1} , indicating that no major alteration in the primary coordination sphere occurred upon removal of the solvent by lyophilization.³⁸ This band was not sensitive to a change of the pH from 5.0 to 7.0.

ESI-MS. Formation of the mercury(II) complexes of CdPPC and CPPC was verified by ESI-MS. Figure 7 (CdPPC) and Figure S6 in the SI (CPPC) show the ESI-MS spectra corresponding to solutions containing 1.0 mM peptide and 1 equiv of Hg^{II} at pH 6.0–6.2. For CdPPC , only the monocharged molecular ions corresponding to the K^+ and Na^+ adducts of the mercury(II) complex were observed

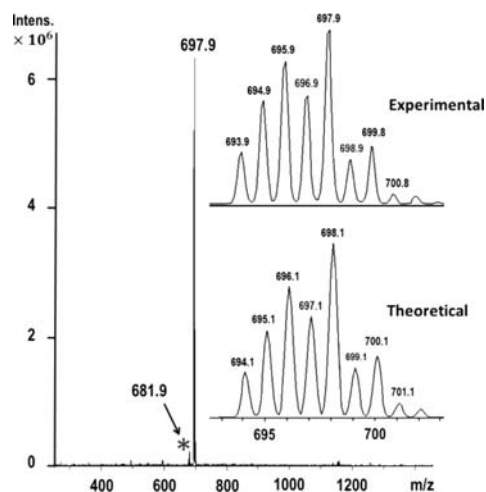


Figure 7. ESI-MS spectrum of the $\text{Hg}(\text{CdPPC})$ complex in the positive mode showing the K^+ ($[\text{Hg}(\text{CdPPC}) + \text{K}^+]^+$, major species) and Na^+ ($[\text{Hg}(\text{CdPPC}) + \text{Na}^+]^+$, minor species, indicated by an asterisk) adducts. The insets show the experimental and theoretical isotopic patterns of the major species ($[\text{Hg}(\text{CdPPC}) + \text{K}^+]^+$).

($[\text{Hg}(\text{CdPPC}) + \text{K}^+]^+ = 697.9$ and $[\text{Hg}(\text{CdPPC}) + \text{Na}^+]^+ = 681.9$). No free peptide was detected. The ESI-MS spectrum recorded for CPPC shows the K^+ adduct of the metal complex ($[\text{Hg}(\text{CPPC}) + \text{K}^+]^+ = 697.9$) and a small peak corresponding to free peptide ($[(\text{CPPC}) + \text{K}^+]^+ = 497.9$).

Potentiometric Studies. The protonation constants of the two peptides and Cys were determined by potentiometric titrations in aqueous solution at 298.2 K and ionic strength 0.10 M in KNO_3 . The data are presented in Table 2. In agreement with the primary sequences of the peptides (acetylated at the N-terminus and amidated at the C-terminus), only two protonation constants were determined corresponding to the thiol groups of the two Cys residues. The values obtained are consistent with those reported in the literature for peptides containing two Cys residues.^{39–41} The three constants obtained for the amino acid Cys can be assigned to the amine (10.03), the thiol (8.08), and the carboxylate (2.00) groups. Spectroscopic studies indicated a strong binding of Hg^{II} to the peptides, and the pH titrations show that the percentage of the mercury(II) complexes formed is too large even at low pH values. Therefore, in order to measure the magnitude of the stability constants of the mercury(II) complexes of the CdPPC and CPPC peptides, competition potentiometric experiments were undertaken using the amino acid Cys as the competitor ligand. First, the overall formation constants (β) for the mercury(II) complexes of Cys were determined under our experimental conditions. Potentiometric data were fit to the species reported in Table 2 using as a fixed value the formation constant reported by Stricks and Kolthoff for the species $[\text{Hg}(\text{Cys}_2)]$.⁴² Afterward, potentiometric titrations were carried out at a 1:1:1 Cys/peptide/mercury(II) ratio. Experimental data were fit using the overall formation constants determined for the complexes of Cys, and the best results were obtained considering the species shown in Table 2. The standard deviations reported for the complexes of the peptides are high because of the slow stabilization observed in the competition region (pH range 7.00–10.00). It was not possible to determine the formation constant of the complex $\text{Hg}(\text{CPPC})$ because Cys is a strong competitor ligand in relation to CPPC . A competitor with a lower affinity for Hg^{II} would be necessary.

Table 2. Overall (β) and Stepwise (K) Protonation Constants of Cys, CdPPC, and CPPC and Formation Constants for the Complexes of These Ligands with Mercury(II) in Aqueous Solution at $T = 298.2 \pm 0.1$ K and $I = 0.10 \pm 0.01$ M in KNO_3

species ^a	Cys		CdPPC		CPPC	
	$\log \beta_i^{\text{H}^b}$	$\log K_i^{\text{H}}$	$\log \beta_i^{\text{H}^b}$	$\log K_i^{\text{H}}$	$\log \beta_i^{\text{H}^b}$	$\log K_i^{\text{H}}$
HL	10.03(1)	10.03	9.39(4)	9.39	9.21(4)	9.21
H ₂ L	18.11(2)	8.08	17.76(4)	8.37	17.60(4)	8.39
H ₃ L	20.11(6)	2.00				
	Cys		CdPPC		CPPC	
	$\log \beta^b$	$\log K$	$\log \beta^b$	$\log K$	$\log \beta^b$	$\log K$
HgCys ₂	43.57 ^c	43.57 ^c				
HgHCys ₂	52.30(2)	8.73				
HgH ₂ Cys ₂	59.79(3)	7.49				
HgH ₃ Cys ₂	62.43(3)	2.64				
HgH ₋₁ Cys ₂	32.57(2)	11.0				
HgL			40.0(5)			
HgCysL			44.2(4)			
HgHCysL			52.7(3)	8.5	45.34(9)	
HgH ₂ CysL					53.6(1)	8.26

^aL indicates the ligand in general, and charges are omitted for simplicity. ^bValues in parentheses are standard deviations in the last significant figure. ^cData from Stricks and Kolthoff.⁴² This value was fixed during the fitting of the potentiometric data in order to obtain the formation constant values for the protonated and hydroxo complexes under our experimental conditions.

The speciation diagram for the system 1:1:1 Cys/CdPPC/mercury(II) ratio is shown in Figure 8. This graphic shows that Hg(CdPPC) is the main species up to pH 8.0 and that mixed species are formed at pH >6.5.

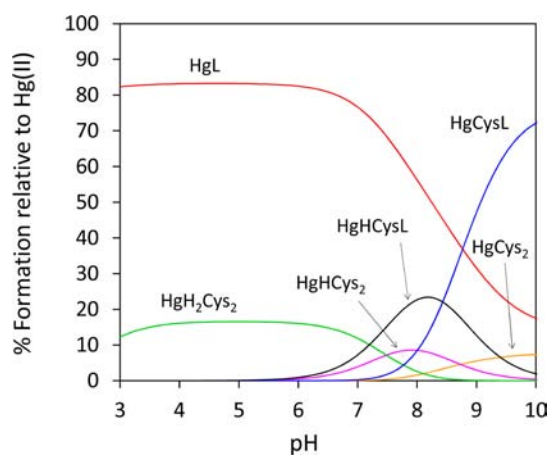


Figure 8. Species distribution diagram for the mercury(II) complexes of the CdPPC peptide in the presence of Cys at a 1:1:1 Cys/CdPPC/mercury(II) ratio (L = CdPPC, and charges are omitted for simplicity). Experimental conditions: 298.2 K, $I = 0.1$ M KNO_3 , and $[\text{Cys}] = [\text{CdPPC}] = [\text{Hg}(\text{NO}_3)_2] = 1.0 \times 10^{-3}$ M.

Computational Modeling. The final optimized conformations at the MP2 level are depicted in Figure 9A,B, and relevant energetic information is shown in Table S1 in the SI. Frequency calculations on the same conformations optimized with B3LYP did not yield any negative eigenvalues in the second derivative matrix, showing that these are minima.

Despite the fact that the electronic and solvation energies would suggest conformer 2 to be the most stable (by -5.85 kJ mol⁻¹), adding thermal energy corrections to the free energy reverts this trend, yielding an energy difference of 3.64 kJ mol⁻¹ favoring conformer 1 (see Table S1 in the SI for details on the calculated energies). Selected structural details of the energy-

minimized structures of the two conformers are given in Table 3.

DISCUSSION

Different peptides have been designed to mimic the loops containing the short amino acid sequence CXXC found in many metalloproteins involved in heavy-metal ion detoxification systems as well as in cellular metal trafficking.¹⁻⁴ Metal ion coordination studies show that they bind Hg^{II} with high affinity and that the Cys positions and overall flexibility of the peptide play a crucial role.¹⁰⁻¹³ Indeed, peptides having some degree of rigidity and thus, preorganizing the binding units, were shown to coordinate Hg^{II} more strongly than unstructured peptides. These results highlight that the metal ion coordinating properties of peptides depend on their ability to adopt well-defined secondary structures that will allow the proper orientation of the side-chain functionalities. This is an important factor affecting not only metal ion coordination but also molecular recognition processes. Therefore, it has driven the design of building blocks, which, upon insertion into short peptide sequences, will induce the formation of specific secondary structures.

One of these building blocks is the dipeptide unit *d*Pro-Pro, the β -turn-inducing properties of which are well-known.¹⁹⁻²¹ It has been used to induce β -sheet and β -hairpin formation upon introduction in short amino acid sequences.²²⁻²⁵ Taking advantage of these properties, this β -turn template was introduced between of two Cys residues to generate the CdPPC peptide and explore its mercury(II) coordination properties. It was hypothesized that this template will preorganize the Cys residues in a favorable manner for proper mercury(II) coordination. The CD spectrum of this peptide in aqueous solution (pH 7.4) shows the features of a type II' β turn with a maximum negative ellipticity at 215 nm,³⁰ which is consistent with the strong tendency of the *d*Pro-Pro motif to adopt this type of secondary structure.^{20,21} The intensity of this CD signal increases upon Hg^{II} binding, suggesting that the peptide adopts a more rigid conformation. Nonetheless, it is difficult to separate the peptide conformation contribution from

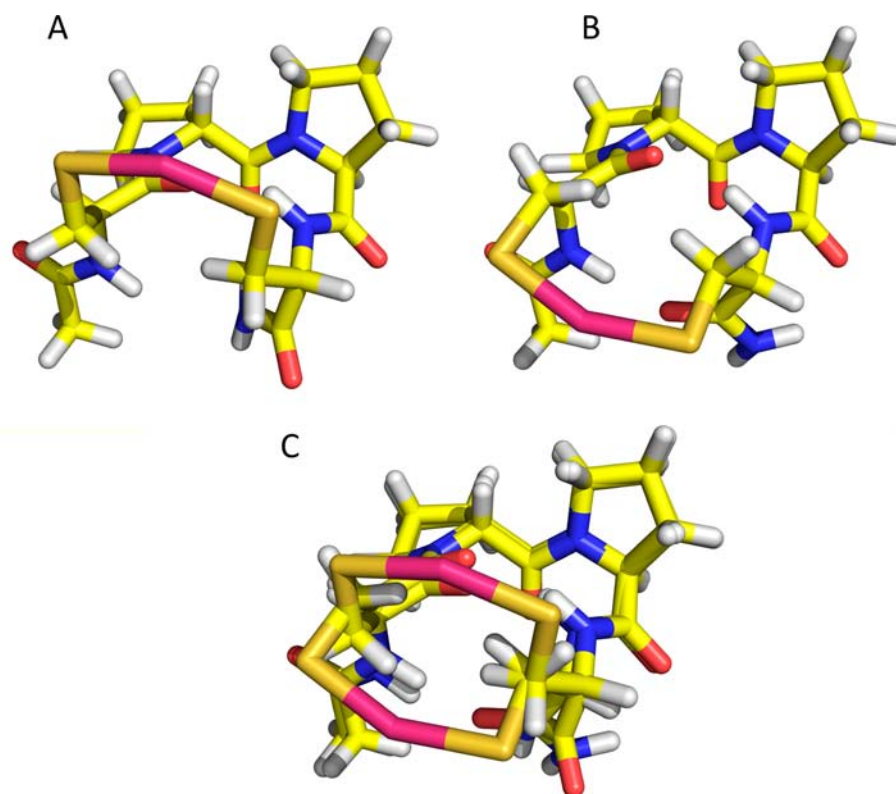


Figure 9. Final optimized (at the MP2 level) conformations of the mercury(II) compound: (A) conformer 1; (B) conformer 2; (C) overlay of the two conformations. The Hg ion is colored pink.

Table 3. Selected Structural Details of the Energy-Minimized Structures

		conformer 1	conformer 2
$R(\text{Hg}-\text{S})$ (Å)	S1	2.42	2.42
	S2	2.44	2.42
distance S-S (Å)		4.74	4.72
angle S-Hg-S (deg)		154.2	153.9
distance Hg-CO (Å)		2.96 (CO-Cys1)	3.45 (CO-Cys2)

that due to LMCT because they occur in the same region. As revealed by CD and UV-vis spectroscopic studies and further confirmed by ESI-MS, the CdPPC peptide forms a mercury(II) complex with 1:1 peptide/mercury(II) stoichiometry. The spectroscopic data of this complex is consistent with that reported for linear dithiolatemercury(II) complexes.^{13,27–29} The CD and UV-vis studies of the pH dependence for the Hg(CdPPC) complex formation reveal that Hg^{II} binds at low pH and remains bound even at very high pH values. Additionally, this complex was stable in solution in the pH range 2.5–9.0 over a period of 36 days. In the absence of Hg^{II}, the CdPPC peptide has a half-life of 16 days at pH 7.4, as determined by using Ellman's test (data not shown).

All of the data described above clearly demonstrate that the CdPPC peptide binds 1 equiv of Hg^{II} with high affinity and suggest that the metal is bound only by the two Cys, forming a dithiolatemercury(II) complex. To confirm this observation and determine the mercury(II) coordination geometry of the complex, ^{199m}Hg PAC and Raman spectroscopies were carried out. ^{199m}Hg PAC spectroscopy has proven to be a powerful tool to determine the number of S atoms bound to Hg^{II} and obtaining structural information.^{33,43,44} The PAC parameters ($\nu_{\text{Q}} = 1.39$ GHz and $\eta = 0.09$; Table 1) obtained at pH 5.1

compare reasonably well with published data for mercury(II) complexes with a distorted linear $[\text{Hg}(\text{RS})_2]$ coordination geometry (Table 4). The slightly lower ν_{Q} observed for this

Table 4. NQI Parameters of Different Distorted Linear Dithiolatemercury(II) Complexes^a

complex	ν_{Q} (GHz)	η	ref
$[\text{Hg}(\text{Cys})_2]$	1.41(2)	0.15(2)	33
MerA (77 K)	1.42(6)	0.15(1)	43
Hg(TRIL9C) ₂	1.529(9) ^b	0.13(3)	44
	1.539(10) ^c	0.11(3)	44

^aNumbers in the parentheses are the standard deviations of the fitted parameters. ^bpH = 6.6. ^cpH = 8.1.

compound compared to the reference compounds may be due to slightly longer Hg-S bond lengths, in agreement with the predictions of computational chemistry, *vide infra*. The PAC parameters of the dominating species showed no major variation with the pH (see Table 1), indicating that a distorted linear Hg(CdPPC) complex is formed in the entire pH range studied. The PAC spectra indicate the presence of a minor species at pH 7.5 and 9.0. This might reflect remote ligands in the equatorial plane of some speciation due to the slight substoichiometric conditions (0.9 Hg^{II} per peptide). Raman difference spectroscopy was employed to identify the band(s) that originate from the vibrational modes that involve the Hg center. The single broad band observed at 325 cm⁻¹ in lyophilized solid samples (Figure 4, trace c) matches data reported in the literature for $\nu_{\text{s}}(\text{Hg}-\text{S})$ of dithiolatemercury(II) complexes.^{34–38} No changes in this band were observed in frozen solution samples in the pH range 5.0–7.0. Overall, the results obtained with ^{199m}Hg PAC and Raman spectroscopies

are consistent with those observed by UV–vis and CD spectroscopic studies.

At this point, it was important to evaluate the effect of the *d*Pro-Pro motif on the mercury(II) coordination properties of the CdPPC peptide, and thus the stereochemical configuration of the *d*Pro was reversed (CPPC peptide). As shown by CD spectroscopy, the CPPC peptide is unstructured (random-coil conformation) in aqueous solution, which confirms the crucial role of *d*Pro in this position to induce a β -turn structure.¹⁹ The CD and UV–vis mercury(II) titrations indicate the formation of a similar 1:1 peptide/mercury(II) complex [Hg(CPPC)], the stoichiometry of which was also confirmed by ESI-MS. Nonetheless, different behaviors were observed for both peptides under excess of Hg^{II} (more than 1 equiv of Hg^{II}). While no major changes are observed for the CdPPC peptide, CD spectroscopy shows that Hg(CPPC) loses its CD signal and the UV–vis spectra show an increase of absorbance in the 240–270 nm spectral window. These data suggest the formation of polymetallic mercury(II) species with concomitant loss of the peptidic structure. The fact that these alterations are not observed for the CdPPC peptide highlights the strong β -turn-inducing character of the *d*Pro-Pro motif^{19–21} and, thus, the formation of a more stable Hg(CdPPC) complex.

To gain some insight into the formation constants ($\log K$) of the mercury(II) complexes, competition potentiometric experiments were carried out using Cys as the competitor ligand. A $\log K = 40.0$ was determined for the formation of the [Hg(CdPPC)] species, which reveals the high affinity of this peptide for Hg^{II}. Under the same conditions, the affinity constant of the CPPC peptide for Hg^{II} could not be determined because this peptidic ligand could not compete with Cys. These results suggest a lower stability constant for the complex Hg(CPPC). Consistent with this observation, the CD and UV–vis spectroscopies showed mainly the formation of Hg(CdPPC) when 1 equiv of Hg^{II} was added to equimolar solutions of both peptides (Figures 2 and 4), indicating that the CPPC peptide binds Hg^{II} with a strength that is at least 3–3.5 orders of magnitude lower ($\log K_{\text{HgL}}$). This difference in binding can be ascribed to the preorganization of the Cys residues by the *d*Pro-Pro unit, an effect that is not present in the unstructured CPPC peptide. As previously observed,¹³ these data indicate that peptides with higher preorganization of the metal binding units can coordinate Hg^{II} with higher affinity. The stability constant of Hg(CdPPC) ($\log \beta = \log K = 40.0$) is much higher than those reported for other peptidic systems containing two Cys,^{11,13} even in the case of preorganized ligands. Nonetheless, it should be pointed out that, in the latest case,¹³ only the lower limit value was reported ($\log \beta > 18.6$), and thus a rigorous comparison cannot be made.

Two possible conformers were geometry optimized for the complex Hg(CdPPC) using quantum-mechanical methods (Figure 9A,B). Both agree with the spectroscopic characteristics reported in this study and thus are not distinguishable by the spectroscopic methods applied. Nonetheless, ¹H NMR spectra obtained at 277.2, 298.2, and 323.15 K seem to indicate the presence of different conformers in solution that interconvert slowly in the NMR time scale (Figure S7 in the SI). In the proposed structures, the Cys are separated by approximately the same distance (4.72–4.74 Å), the bond lengths (Hg–S) are approximately the same (2.42–2.44 Å), and the angle S–Hg–S is 154.2° vs 153.9° (Table 3). Considering that the average bond lengths reported for Hg(RS)₂ and Hg(RS)₃ complexes are 2.345 ± 0.025 and 2.446 ± 0.018 Å, respectively,⁴⁵ our

energy-minimized structures show an intermediate bond length. The optimized structure of the model complex Hg(SCH₃)₂ using the same methodology gives a Hg–S distance of 2.40 Å and an angle S–Hg–S of 178.5°, making it essentially linear. These values are very similar to those reported for the crystal structure of the model complex.⁴⁶ Thus, the coordination geometry in our complex is strained by the loop motif and possibly by interactions with the carbonyl group, bending the S–Hg–S unit and slightly increasing the bond length. Similar contacts in the equatorial plane are observed for other Hg^{II}-containing compounds with a coordination number of 2.²⁷ It is noteworthy that the binding of Hg^{II} to the peptide remains strong despite the substantial deviation from a linear S–Hg–S structure. The major differences between the two conformers are the orientation of the plane containing S–Hg–S with respect to the anchoring C atoms and thus to the rest of the peptide (Figure 9C). In addition, the hydrogen-bond pattern differs, and consequently, the weak interaction with the carbonyl group (CO of the first Cys in conformer 1 and CO of the second Cys in conformer 2). Because the proposed structures for both conformers are based on theoretical calculations, we cannot rule out the existence of other structures in solution.

CONCLUSION

In summary, a short CdPPC peptide has been designed, mimicking the CXXC chelating unit and containing the template *d*Pro-Pro unit to adopt a preorganized structure (β -turn). Spectroscopic and ESI-MS studies show that this short peptide binds Hg^{II} with high affinity ($\log K = 40.0$), forming a mononuclear dithiolatemercury(II) complex Hg(CdPPC). pH-dependent studies reveal that the complex is stable over a wide pH range and over time. The replacement of the *d*Pro-Pro motif by the Pro-Pro unit generates a peptide (CPPC) that is unstructured and binds Hg^{II} with a lower affinity. While the simple *d*Pro-Pro template mimics the overall preorganization achieved by the protein scaffold in CXXC containing metalloproteins, the known high thiophilicity of mercury stabilizes the final construct in a wide pH range. We are currently exploring and developing modifications of this small system for the design of mercury(II) chelators/sensors. This short peptide, acetylated at the N-terminus and amidated at the C-terminus, allows structural modifications without changes in the positions of the Cys binding units. Additionally, this robust metal stabilized turn may have important implications in protein design to obtain pH stable β -sheet and β -hairpin structures. Recently, it has been shown that the binding of Hg^{II} to Cys containing coiled coils can stabilize their final structure in a wider pH range.⁴⁷

EXPERIMENTAL SECTION

Chemicals. The *N*-fluorenylmethoxycarbonyl (Fmoc)-protected amino acids (Fmoc-Cys-OH, Fmoc-D-Pro-OH, and Fmoc-Pro-OH), 2-(1*H*-benzotriazol-1-yl)-1,1,3,3-tetramethyluronium hexafluorophosphate (HBTU), and the MBHA rink amide resin were obtained from Novabiochem; *N,N*-diisopropylethylamine (DIEA), piperidine, anisole, thioanisole, 1,2-ethanedithiol, Hg(NO₃)₂, and HgCl₂ were purchased from Sigma-Aldrich; trifluoroacetic acid (TFA) was obtained from Roth; diethyl ether and 85% phosphoric acid were obtained from Panreac; dipotassium hydrogen phosphate and potassium dihydrogen phosphate were obtained from PROLABO. All other chemicals and solvents [*N,N*-dimethylformamide (DMF), dichloromethane, acetonitrile (ACN), *N*-methyl-2-pyrrolidone, and

acetic anhydride (Ac_2O)] were from different commercial sources (highest available grade) and were used without further purification.

Peptide Synthesis and Purification. The peptides Ac-Cys-dPro-Pro-Cys-NH₂ (CdPPC) and Ac-Cys-Pro-Pro-Cys-NH₂ (CPPC) were synthesized in a Liberty Automated Peptide Synthesizer on a 0.5 mmol scale using standard Fmoc protocols.²⁶ The MBHA rink amide resin was used as a solid support, resulting in the C-terminus amidation of the peptide product, the activation method employed was HBTU/DIEA, and the N-terminus was acetylated at the end of the synthesis using a solution of 20% Ac_2O in DMF. Cleavage from the resin and removal of the protecting groups were performed simultaneously by treatment with a mixture of TFA/anisole/thioanisole/1,2-ethanedithiol (% v/v = 90:2:5:3) for 2 h at room temperature and under nitrogen. The solution containing the free peptide was filtered in order to remove the resin and washed with TFA. The solution was then concentrated under a nitrogen stream, and cold diethyl ether was added to precipitate the crude peptide. The solid was redissolved in 10% acetic acid and purified by reverse-phase HPLC. HPLC was performed using a Beckman System Gold instrument equipped with a programmable solvent module 126, a scanning detector module 167, and a Phenomenex Jupiter 15 μm C18 300 Å column (250 \times 10 mm). The following linear gradient at a flow rate of 4 mL min⁻¹ was used: 0–100% solvent B in 30 min [solvent A = water/TFA (% v/v = 100:0.01) and solvent B = water/ACN/TFA (% v/v = 10:90:0.01)]. The identity of the peptides was verified by ESI-MS: m/z 460.2 ($[\text{M} + \text{H}]^+$) and 482.3 ($[\text{M} + \text{Na}]^+$) (Figure S1 in the SI); the results are in agreement with the calculated $[\text{M} + \text{H}]^+ = 460.2$ Da and $[\text{M} + \text{Na}]^+ = 482.2$ Da. The purity (>95%) was determined by analytical HPLC using a Phenomenex Jupiter Proteo 4 μm 90 Å column (250 \times 4.6 mm).

Stock Solutions. The peptide stock solutions were prepared freshly prior to each experiment using Milli-Q water previously purged with argon to minimize oxidation. The peptide concentration was determined by quantification of the cysteine thiols using Ellman's test,⁴⁸ which uses dithionitrobenzoate as an indicator. The HgCl_2 and $\text{Hg}(\text{NO}_3)_2$ stock solutions were prepared from analytical-grade metal salt and the exact concentrations determined by standard complexometric procedures using ethylenediaminetetraacetic acid (EDTA)⁴⁹ and/or by inductively coupled plasma atomic emission spectroscopy. The latter experiments were performed in the Analytical Laboratory of the Chemistry Department at the Faculdade de Ciências e Tecnologia, Universidade Nova de Lisboa.

Spectroscopic Studies. UV-Vis Spectroscopy. All of the UV-vis spectra were acquired at 25 °C on a Varian Cary 100 Bio UV-vis spectrophotometer equipped with a thermostatted multiple-cell holder and a Peltier water bath using 1-cm-path-length quartz cells.

Metal Binding. Hg^{II} binding studies were performed by titrating aliquots of a 10.4 mM HgCl_2 stock solution into a 2.5 mL solution containing 25 μM peptides and 20.0 mM appropriate buffer. For each mercury addition, an equivalent addition was made in the reference cell containing only 20.0 mM appropriate buffer, so that the difference spectrum taken was only attributed to the binding of Hg^{II} to the peptide. No equilibration time after each metal aliquot addition was required because the UV-vis spectrum recorded 1 min after each metal aliquot addition was exactly the same as that obtained after 15 min of equilibration. Therefore, all of the spectra were recorded 1 min after Hg^{II} addition. The development of the LMCT band corresponding to the binding of Hg^{II} to Cys was monitored between 190 and 350 nm. The pH of the solution was measured after the experiment, and it was always within 0.05 pH units of the initial pH value.

UV-Vis pH Titrations. These experiments were performed by adding small aliquots of 1.0 mM to 1.0 M solutions of potassium hydroxide or hydrochloric acid to unbuffered solutions containing 25 μM metal salt and 25 μM peptide and monitoring the change in the absorbance spectrum as a function of the pH. An equilibration time was always allowed before the final pH was read, which was measured using a mini-glass combination pH electrode (Hamilton Biotrode) coupled to a Crison BASIC 20+ digital pH meter. Although special

care was taken to reduce as much as possible the contact with O_2 , the samples were exposed to O_2 during pH adjustments.

Peptide and Hg(CdPPC) Complex Stability Studies. Solutions containing 25 μM CdPPC and 20.0 mM appropriate buffer (phosphoric acid buffer for pH 2.5, phosphate buffer for pH 7.4, and CHES buffer for pH 9.0) were prepared and the concentrations of free thiols determined over time by Ellman's test.⁴⁴ Solutions containing a 25 μM $\text{Hg}(\text{CdPPC})$ complex and 20.0 mM appropriate buffer (same as above) were prepared and monitored over time by UV-vis spectroscopy.

CD Spectroscopy. All CD spectroscopic experiments were performed at 25 °C under a constant flow of nitrogen on a Jasco J-715 spectropolarimeter equipped with a thermostatted cell holder and a Peltier bath using a 1-cm-path-length quartz cell. CD spectra were collected in the wavelength range from 190 to 350 nm using the following parameters: standard sensitivity = 100 mdeg; continuous scanning mode at a speed of 200 nm min⁻¹; bandwidth = 2 nm; accumulation = 8 scans. When buffers were not used, an equilibration time was always allowed before the final pH was read.

Metal Binding. The metal binding titrations at pH 7.4 were performed by titrating aliquots of a 10.4 mM HgCl_2 stock solution into a 2.0 mL unbuffered solution containing 10 μM peptide CdPPC and adjusting the pH value by adding small aliquots of 1.0 mM to 1.0 M solutions of potassium hydroxide and/or hydrochloric acid. For CPPC peptide, these experiments were carried out using 20 μM peptide in 5.0 mM phosphate buffer.

CD pH Titrations. The pH titrations were performed by adding small aliquots of 1.0 mM to 1.0 M solutions of potassium hydroxide and/or hydrochloric acid to unbuffered solutions containing 5.0 μM HgCl_2 and 5.0 μM peptide CdPPC.

For all of the CD spectra, the molar ellipticity, $[\theta]$, is given in units of deg cm² dmol⁻¹ and was calculated using eq 1, where θ_{obs} is the ellipticity in millidegrees, l is the path length of the cell in centimeters, and C is the peptide concentration in moles per liter. The difference CD spectra are reported with molar ellipticities referenced to the total peptide concentration.

$$\theta = \frac{\theta_{\text{obs}}}{10lC} \quad (1)$$

^{199m}Hg PAC Spectroscopy. The production of ^{199m}Hg and data collection were performed at CERN as previously reported.⁴⁴ The following stock solutions were prepared and used for these experiments: 10.4 mM and 318 μM CdPPC peptide (as determined by Ellman's test),⁴⁸ 333.0 mM acetate buffer (pH 5.0), 333.0 mM phosphate buffer (pH 8.0), and 333.0 mM CHES buffer (pH 10.0). The final samples for the ^{199m}Hg PAC experiments contained 25 μM peptide, 22.5 μM $\text{Hg}(\text{CH}_3\text{COO})_2$, and 35.0 mM appropriate buffer. The PAC instrument was described previously,⁵⁰ and the time resolution and calibration were determined to be 0.736 ns and 0.0504 ns per channel, respectively. The experiments were done at 77 K to eliminate rotational diffusion. All of the fits were carried out with 300 points, disregarding the first 5 points due to systematic errors. Each NQI was modeled by using a separate set of parameters that included ν_{Q} , η , δ , $1/\tau_{\text{Q}}$, and A (see ref 51 for a detailed description of the parameters).

Raman Spectroscopy. Raman spectra were measured in back-scattering geometry using a confocal microscope coupled to a Raman spectrometer (Jobin Yvon U1000) equipped with a 1200 mm⁻¹ grating and a liquid-nitrogen-cooled CCD detector. An Olympus 20 \times objective with a working distance of 21 mm and a numeric aperture of 0.35 was used. A total of 4 μL of 0.237 M solutions of the CdPPC peptide and $\text{Hg}(\text{CdPPC})$ complex, at pH 7.4 and 5.0, was placed in a liquid-nitrogen-cooled cryostat (Linkam THMS600). Additionally, solid lyophilized samples were measured using the same setup. Raman spectra were recorded at 83 K with the 413 nm line from a Kr^+ -ion laser (Coherent Innova 302), 7.5 mW laser power, and an accumulation time of 60 s. For each sample, 20–80 spectra were coadded to obtain a satisfactory signal-to-noise ratio. Spectra of the peptide were subtracted from those of the mercury peptide samples using homemade software.⁵²

ESI-MS. ESI-MS spectra were acquired on a Bruker Daltonics Esquire 3000 plus mass spectrometer equipped with an API source. The source temperature was set to 250 °C, nitrogen was used as a drying gas at a flow rate of 5 L min⁻¹ and at a constant pressure of 15 psi, and samples were infused at a flow rate of 5 μL min⁻¹.

Potentiometric Studies. Purified water was obtained from a Millipore Milli-Q demineralization system. Stock solutions of CdPPC and CPPC were prepared in the range (3.0–9.0) × 10⁻³ M and of Cys at 2.4 × 10⁻³ M (cysteine chloride was purchased from Merck). A Hg^{II} ion solution was prepared in 0.018 M HNO₃ at 0.0254 M from analytical-grade nitrate salts of the metal ion and standardized by titration with Na₂H₂EDTA.⁵³ Carbonate-free solutions of the titrant KOH were obtained at 0.106 M by a freshly prepared solution from a Merck ampule in 1000 mL of water (freshly boiled for about 2 h and allowed to cool under nitrogen). These solutions were standardized by application of Gran's method⁵⁴ and discarded as soon as the concentration of carbonate reached ca. 1% of the total amount of base. A 0.100 M standard solution of HNO₃ prepared from a commercial ampule was used for backtitrations. The potentiometric setup used for conventional titrations consisted of a 50 mL glass-jacketed titration cell sealed from the atmosphere and connected to a separate glass-jacketed reference electrode cell by a Wilhelm-type salt bridge containing a 0.10 M KNO₃ solution. An Orion 720A measuring instrument fitted with a Metrohm 6.0123.100 glass electrode and an Orion 95-05-00 Ag/AgCl reference electrode was used for the measurements. Titrant solutions were added through capillary tips at the surface of the experimental solution by a Metrohm Dosimat 665 automatic buret. The titration procedure is automatically controlled by software after selection of suitable parameters, allowing for long unattended experimental runs. [H⁺] of the solutions was determined by measurement of the electromotive force of the cell, $E = E^{o'} + Q \log [H^+] + E_j$. The term pH is defined as $-\log [H^+]$. $E^{o'}$, and Q was determined by titrating a solution of known H-ion concentration at the same ionic strength in the acidic pH region. The liquid-junction potential, E_j , was found to be negligible under the experimental conditions used. The value of $K_w = [H^+][OH^-]$ was found to be equal to 10^{-13.77} by titrating a solution of known H-ion concentration at the same ionic strength in the alkaline pH region, considering $E^{o'}$ and Q as valid for the entire pH range. The ionic strength of the experimental solutions was kept at 0.10 M with KNO₃, and the temperature was controlled at 298.2 ± 0.1 K using a Grant W6/CZ1 thermostatic system. All of the experiments were performed using a total volume of 30 mL and under argon to avoid possible oxidation of Cys. Measurements to determine the protonation constants were carried out with ca. 0.03 mmol of ligand. The Cys–Hg^{II} complexation was performed with ca. 0.06 mmol of Cys and 0.03 mmol of Hg^{II}. Competition experiments were carried out with ca. 0.03 mmol of peptide in the presence of 1 equiv of Cys and 1 equiv of Hg^{II}, and 1 h of equilibration time was allowed before the titrations were started. A backtitration was always performed at the end of each direct complexation titration in order to check whether equilibrium was attained throughout the full pH range. Each titration curve consisted typically of 80–100 points in the 3–11 pH region, and a minimum of two replicate titrations were performed for each system.

Calculation of the Equilibrium Constants. Calculation of the overall equilibrium constants β_i^H and β_{MmHhLi} (with $\beta_{MmHhLi} = [M_m H_h L_i] / [M]^m [H]^h [L]^i$) was done by fitting the potentiometric data from protonation or complexation titrations with the HYPERQUAD program.⁵⁵ Differences, in log units, between the values of protonated or hydrolyzed and nonprotonated constants provide the stepwise reaction constants. The errors quoted are the standard deviations of the overall stability constants calculated by the fitting program from the experimental data and conditions used. The species distribution diagram was plotted from the calculated constants with the HYSS program.⁵⁶

Computational Modeling. The starting structures for the calculations were modeled from the X-ray structure of pivaloyl-D-Pro-L-Pro-L-Ala-N-methylamide,²¹ which consists of a β turn. During building of the two Cys side chains bound to the Hg, we realized that

two conformations could be built. The first, conformation 1, contains the Hg outside of the plane formed by the β turn, while the second, conformation 2, contains the Hg more or less within this plane. Both conformations were energy-optimized at the MP2 level, using the 6-31G(d,p) basis set for organic atoms and the SDD effective core potential for the Hg atom. This level of theory and basis set combination is a trade-off between the computational time and geometric accuracy, as analyzed by comparing several methods with high-level calculations done with CCSD and the cc-pVTZ basis (SDD for Hg) for a linear mercury thiolate [Hg(SCH₃)₂] (results not shown). *Gaussian 09* was used for all calculations.⁵⁷ The calculations were done considering water as a solvent and the IEFPCM method. B3LYP (with optimization) was used instead of MP2 to calculate thermal energy corrections to the free energy and to verify that the conformations corresponded to minima.

■ ASSOCIATED CONTENT

■ Supporting Information

ESI-MS spectra of the peptides and Hg(CPPC), UV–vis and CD pH titrations of Hg^{II} binding to CdPPC, UV–vis and CD Hg^{II} titrations for CPPC, ¹H NMR spectra, and calculated energies for the two conformers of the complex Hg(CdPPC). This material is available free of charge via the Internet at <http://pubs.acs.org>.

■ AUTHOR INFORMATION

Corresponding Author

*E-mail: oiranzo@itqb.unl.pt.

Notes

The authors declare no competing financial interest.

■ ACKNOWLEDGMENTS

This work was carried out with financial support from the Fundação para a Ciência e a Tecnologia (Grant PTDC/QUI-QUI/105504/2008 to O.L., postdoctoral fellowship PTDC/BIA-PRO/100791/2008 to M.S., National Mass Spectrometry (REDE/1504/REM/2005) and NMR (REDE/1517/RMN/2005) Networks, and Pest-OE/EQB/LA0004/2011), and from the Danish Research Council (DFFIFNU) and with beamtime at ISOLDE CERN (IS488) to L.H. The authors thank Prof. Rita Delgado for her guidance in the potentiometric studies and a discussion of the data, Dr. Smilja Todorovic for the Raman spectroscopic data, and M. C. Almeida for the ESI-MS spectra.

■ REFERENCES

- (1) Rosenzweig, A. C. *Acc. Chem. Res.* **2000**, *34*, 119.
- (2) Opella, S. J.; DeSilva, T. M.; Veglia, G. *Curr. Opin. Chem. Biol.* **2002**, *6*, 217.
- (3) Puig, S.; Thiele, D. J. *Curr. Opin. Chem. Biol.* **2002**, *6*, 171.
- (4) Shoshan, M. S.; Tshuva, E. Y. *Chem. Soc. Rev.* **2011**, *40*, 5282.
- (5) Steele, R. A.; Opella, S. J. *Biochemistry* **1997**, *36*, 6885.
- (6) Klomp, L. W. J.; Lin, S.-J.; Yuan, D. S.; Klausner, R. D.; Culotta, V. C.; Gitlin, J. D. *J. Biol. Chem.* **1997**, *272*, 9221.
- (7) Pufahl, R. A.; Singer, C. P.; Peariso, K. L.; Lin, S.-J.; Schmidt, P. J.; Fahrni, C. J.; Culotta, V. C.; Penner-Hahn, J. E.; O'Halloran, T. V. *Science* **1997**, *278*, 853.
- (8) Wimmer, R.; Herrmann, T.; Solioz, M.; Wüthrich, K. *J. Biol. Chem.* **1999**, *274*, 22597.
- (9) Yamamura, T.; Watanabe, T.; Kikuchi, A.; Ushiyama, M.; Kobayashi, T.; Hirota, H. *J. Phys. Chem.* **1995**, *99*, 5525.
- (10) Veglia, G.; Porcelli, F.; DeSilva, T.; Prantner, A.; Opella, S. J. *J. Am. Chem. Soc.* **2000**, *122*, 2389.
- (11) DeSilva, T. M.; Veglia, G.; Porcelli, F.; Prantner, A. M.; Opella, S. J. *Biopolymers* **2002**, *64*, 189.
- (12) Seneque, O.; Crouzy, S.; Boturyn, D.; Dumy, P.; Ferrand, M.; Delangle, P. *Chem. Commun.* **2004**, 770.

- (13) Rousselot-Pailley, P.; Sénèque, O.; Lebrun, C.; Crouzy, S.; Boturyn, D.; Dumy, P.; Ferrand, M.; Delangle, P. *Inorg. Chem.* **2006**, *45*, 5510.
- (14) Luczkowski, M.; Stachura, M.; Schirf, V.; Demeler, B.; Hemmingsen, L.; Pecoraro, V. L. *Inorg. Chem.* **2008**, *47*, 10875.
- (15) Niedźwiecka, A.; Cisnetti, F.; Lebrun, C.; Delangle, P. *Inorg. Chem.* **2012**, *51*, 5458.
- (16) Imperiali, B.; Kapoor, T. M. *Tetrahedron* **1993**, *49*, 3501.
- (17) Cheng, R. P.; Fisher, S. L.; Imperiali, B. *J. Am. Chem. Soc.* **1996**, *118*, 11349.
- (18) Daugherty, R. G.; Wasowicz, T.; Gibney, B. R.; DeRose, V. J. *Inorg. Chem.* **2002**, *41*, 2623.
- (19) Bean, J. W.; Koppale, K. D.; Peishoff, C. E. *J. Am. Chem. Soc.* **1992**, *114*, 5328.
- (20) Chalmers, D. K.; Marshall, G. R. *J. Am. Chem. Soc.* **1995**, *117*, 5927.
- (21) Nair, C. M.; Vijayan, M.; Venkatachalapathi, Y. V.; Balaram, P. *J. Chem. Soc., Chem. Commun.* **1979**, 1183.
- (22) Späth, J.; Stuart, F.; Jiang, L.; Robinson, J. A. *Helv. Chim. Acta* **1998**, *81*, 1726.
- (23) Sénèque, O.; Bourlès, E.; Lebrun, V.; Bonnet, E.; Dumy, P.; Latour, J.-M. *Angew. Chem., Int. Ed.* **2008**, *47*, 6888.
- (24) Robinson, J. A. *Acc. Chem. Res.* **2008**, *41*, 1278.
- (25) Schneider, J. P.; Pochan, D. J.; Ozbas, B.; Rajagopal, K.; Pakstis, L.; Kretsinger, J. *J. Am. Chem. Soc.* **2002**, *124*, 15030.
- (26) Chan, W. C.; White, P. D. *Fmoc Solid Phase Peptide Synthesis*; Oxford University Press: Oxford, NY, 2000; Vol. 222.
- (27) Wright, J. G.; Natan, M. J.; MacDonnell, F. M.; Ralston, D. M.; O'Halloran, T. V. In *Progress in Inorganic Chemistry: Bioinorganic Chemistry*; Lippard, S. J., Ed.; John Wiley & Sons, Inc.: New York, 1990; Vol. 38, p 323.
- (28) Dieckmann, G. R.; McRorie, D. K.; Tierney, D. L.; Utschig, L. M.; Singer, C. P.; O'Halloran, T. V.; Penner-Hahn, J. E.; DeGrado, W. F.; Pecoraro, V. L. *J. Am. Chem. Soc.* **1997**, *119*, 6195.
- (29) Iranzo, O.; Ghosh, D.; Pecoraro, V. L. *Inorg. Chem.* **2006**, *45*, 9959.
- (30) Rose, G. D.; Gierasch, L. M.; Smith, J. A. *Adv. Protein Chem.* **1985**, *37*, 1.
- (31) Rao, B. N. N.; Kumar, A.; Balaram, H.; Ravi, A.; Balaram, P. *J. Am. Chem. Soc.* **1983**, *105*, 7423.
- (32) Kishore, R.; Raghobama, S.; Balaram, P. *Biochemistry* **1988**, *27*, 2462.
- (33) Butz, T.; Tröger, W.; Pohlmann, T.; Nuyken, O. *Z. Naturforsch., A: Phys. Sci.* **1992**, *47*, 85.
- (34) Utschig, L. M.; Wright, J. G.; O'Halloran, T. V. In *Methods in Enzymology*; James, F. R., Bert, L. V., Eds.; Academic Press: New York, 1993; Vol. 226, p 71.
- (35) Bowmaker, G. A.; Dance, I. G.; Harris, R. K.; Henderson, W.; Laban, I.; Scudder, M. L.; Oh, S.-W. *J. Chem. Soc., Dalton Trans.* **1996**, 2381.
- (36) Fleissner, G.; Kozłowski, P. M.; Vargel, M.; Bryson, J. W.; O'Halloran, T. V.; Spiro, T. G. *Inorg. Chem.* **1999**, *38*, 3523.
- (37) Hoffmann, G. G.; Brockner, W.; Steinfatt, I. *Inorg. Chem.* **2001**, *40*, 977.
- (38) Jalilehvand, F.; Leung, B. O.; Izadifard, M.; Damian, E. *Inorg. Chem.* **2006**, *45*, 66.
- (39) Vogler, R.; Gelinsky, M.; Guo, L. F.; Vahrenkamp, H. *Inorg. Chim. Acta* **2002**, *339*, 1.
- (40) Kulon, K.; Woźniak, D.; Wegner, K.; Grzonka, Z.; Kozłowski, H. *J. Inorg. Biochem.* **2007**, *101*, 1699.
- (41) Krzywoszynska, K.; Rowinska-Zyrek, M.; Witkowska, D.; Potocki, S.; Luczkowski, M.; Kozłowski, H. *Dalton Trans.* **2011**, *40*, 10434.
- (42) Stricks, W.; Kolthoff, I. M. *J. Am. Chem. Soc.* **1953**, *75*, 5673.
- (43) Tröger, W. *Hyperfine Interact.* **1999**, *120/121*, 117.
- (44) Iranzo, O.; Thulstrup, P. W.; Ryu, S.-b.; Hemmingsen, L.; Pecoraro, V. L. *Chem.—Eur. J.* **2007**, *13*, 9178.
- (45) Manceau, A.; Nagy, K. L. *Dalton Trans.* **2008**, 1421.
- (46) Bradley, D. C.; Kunchur, N. R. *J. Chem. Phys.* **1964**, *40*, 2258.
- (47) Zastrow, M. L.; Peacock Anna, F. A.; Stuckey, J. A.; Pecoraro, V. L. *Nat. Chem.* **2012**, *4*, 118.
- (48) Ellman, G. L. *Arch. Biochem. Biophys.* **1959**, *82*, 70.
- (49) *Handbook of Analytical Chemistry*; McGraw-Hill: New York, 1963; Vol. 1.
- (50) Butz, T.; Saibene, S.; Fraenzke, T.; Weber, M. *Nucl. Instrum. Methods Phys. Res., Sect. A* **1989**, *284*, 417.
- (51) Hemmingsen, L.; Sas, K. N.; Danielsen, E. *Chem. Rev.* **2004**, *104*, 4027.
- (52) QPipsi, developed by Uwe Hoffmann (uwe.hoffmann@nir-tools.de).
- (53) Schwarzenbach, G.; Flaschka, W. *Complexometric Titrations*; Methuen & Co.: London, 1969.
- (54) Rossotti, F. J. C.; Rossotti, H. *J. Chem. Educ.* **1965**, *42*, 375.
- (55) Gans, P.; Sabatini, A.; Vacca, A. *Talanta* **1996**, *43*, 1739.
- (56) Alderighi, L.; Gans, P.; Ienco, A.; Peters, D.; Sabatini, A.; Vacca, A. *Coord. Chem. Rev.* **1999**, *184*, 311–318.
- (57) Frisch, M. J.; Trucks, G. W.; Schlegel, H. B.; Scuseria, G. E.; Robb, M. A.; Cheeseman, J. R.; Scalmani, G.; Barone, V.; Mennucci, B.; Petersson, G. A.; Nakatsuji, H.; Caricato, M.; Li, X.; Hratchian, H. P.; Izmaylov, A. F.; Bloino, J.; Zheng, G.; Sonnenberg, J. L.; Hada, M.; Ehara, M.; Toyota, K.; Fukuda, R.; Hasegawa, J.; Ishida, M.; Nakajima, T.; Honda, Y.; Kitao, O.; Nakai, H.; Vreven, T.; Montgomery, J. A., Jr.; Peralta, J. E.; Ogliaro, F.; Bearpark, M.; Heyd, J. J.; Brothers, E.; Kudin, K. N.; Staroverov, V. N.; Kobayashi, R.; Normand, J.; Raghavachari, K.; Rendell, A.; Burant, J. C.; Iyengar, S. S.; Tomasi, J.; Cossi, M.; Rega, N.; Millam, N. J.; Klene, M.; Knox, J. E.; Cross, J. B.; Bakken, V.; Adamo, C.; Jaramillo, J.; Gomperts, R.; Stratmann, R. E.; Yazyev, O.; Austin, A. J.; Cammi, R.; Pomelli, C.; Ochterski, J. W.; Martin, R. L.; Morokuma, K.; Zakrzewski, V. G.; Voth, G. A.; Salvador, P.; Dannenberg, J. J.; Dapprich, S.; Daniels, A. D.; Farkas, Ö.; Foresman, J. B.; Ortiz, J. V.; Cioslowski, J.; Fox, D. J. *Gaussian 09*; Gaussian, Inc.: Wallingford, CT, 2009.